J|A|C|S
ARTICLES
Published on Web 10/05/2004

Dopant Ion Size and Electronic Structure Effects on Transparent Conducting Oxides. Sc-Doped CdO Thin Films Grown by MOCVD

Shu Jin,[†,‡] Yu Yang,[†,‡] Julia E. Medvedeva,[‡,§] John R. Ireland,[∥] Andrew W. Metz,[†,‡] Jun Ni,[†,‡] Carl R. Kannewurf,[∥] Arthur J. Freeman,*[,‡,§] and Tobin J. Marks*[,†,‡]

Contribution from the Department of Chemistry, Materials Research Center, Department of Physics and Astronomy, and Department of Electrical and Computer Engineering, Northwestern University, Evanston, Illinois 60208-3113

Received May 31, 2004; E-mail: t-marks@northwestern.edu; art@freeman.phys.northwestern.edu

Abstract: A series of Sc-doped CdO (CSO) thin films have been grown on both amorphous glass and single-crystal MgO(100) substrates at 400 °C by MOCVD. Both the experimental data and theoretical calculations indicate that Sc^{3+} doping shrinks the CdO lattice parameters due to its relatively small six-coordinate ionic radius, 0.89 Å, vs 1.09 Å for Cd^{2+}. Conductivities as high as 18100 S/cm are achieved for CSO films grown on MgO(100) at a Sc doping level of 1.8 atom %. The CSO thin films exhibit an average transmittance >80% in the visible range. Sc^{3+} doping widens the optical band gap from 2.7 to 3.4 eV via a Burstein−Moss energy level shift, in agreement with the results of band structure calculations within the sX-LDA (screened-exchange local density approximation) formalism. Epitaxial CSO films on single-crystal MgO(100) exhibit significantly higher mobilities (up to 217 $cm^2/(V\cdot s)$) and carrier concentrations than films on glass, arguing that the epitaxial CSO films possess fewer scattering centers and higher doping efficiencies due to the highly textured microstructure. Finally, the band structure calculations provide a microscopic explanation for the observed dopant size effects on the structural, electronic, and optical properties of CSO.

Introduction

Transparent conducting oxides (TCOs), a fascinating class of materials that are both optically transparent and electrically conductive, are finding increasing application in optoelectronic devices such as flat panel displays (FPDs), OLEDs, photovoltaics, solar cells, heat reflectors, de-icers, and energy-efficient windows. Advances in all of these technologies would greatly benefit from new TCO materials with, among other characteristics, greater charge transport capacities and broader transparency windows.[1−3] Recently, CdO-based TCOs received much attention due to their exceptional carrier mobilities, nearly metallic conductivities, and relatively simple crystal structures.[2,4−7] Sn doping of CdO thin films grown epitaxially on MgO(111) by pulsed laser deposition (PLD) achieved thin film mobilities and conductivities as high as 607 $cm^2/(V\cdot s)$ and 42000 S/cm, respectively, rendering them the most conductive TCO thin films with the highest carrier mobilities grown to date.[7] In addition, Cd_2SnO_4, $CdIn_2O_4$, and CdO−ZnO thin films have been grown with good to excellent conductivities (up to 8300 S/cm) and excellent optical transparencies (band gaps as large as 3.7 eV) for photovoltaic applications.[3,8] Although the optical band gap of pure bulk CdO is only 2.3 eV,[9] leading to relatively poor optical transparency in the short-wavelength range, aliovalent metal doping offers the possibility of tuning the electronic structure and the optical band gap through a carrier concentra-

[†] Department of Chemistry.
[‡] Materials Research Center.
[§] Department of Physics and Astronomy.
[∥] Department of Electrical and Computer Engineering.

(1) (a) Freeman, A. J.; Poeppelmeier, K. R.; Mason, T. O.; Chang, R. P. H.; Marks, T. J. *MRS Bull.* **2000**, *25*, 45. (b) Kawazoe, H.; Yanagi, H.; Ueda, K.; Hosono, H. *MRS Bull.* **2000**, *25*, 28. (c) Lewis, B. G.; Paine, D. C. *MRS Bull.* **2000**, *25*, 22. (d) Minami, T. *MRS Bull.* **2000**, *25*, 38. (e) Gordon, R. G. *MRS Bull.* **2000**, *25*, 52. (f) Granqvist, C. G.; Hultaker, A. *Thin Solid Films* **2002**, *411*, 1. (g) Hosono, H.; Ohta, H.; Orita, M.; Ueda, K.; Hirano, M. *Vacuum* **2002**, *66*, 419. (h) Coutts, T. J.; Young, D. L.; Li, X. *MRS Bull.* **2000**, *25*, 58.

(2) (a) Ginley, D. S.; Bright, C. *MRS Bull.* **2000**, *25*, 15. (b) Mason, T. O.; Gonzalez, G. B.; Kammler, D. R.; Mansourian-Hadavi, N.; Ingram, B. J. *Thin Solid Films* **2002**, *411*, 106.

(3) (a) Wu, X.; Dhere, R. G.; Albin, D. S.; Gessert, T. A.; DeHart, C.; Keane, J. C.; Duda, A.; Coutts, T. J.; Asher, S.; Levi, D. H.; Moutinho, H. R.; Yan, Y.; Moriarty, T.; Johnston, S.; Emery, K.; Sheldon, P. *Proc.—NCPV Program Rev. Meet., Lakewood, Co, USA* **2001**, 47. (b) Coutts, T. J.; Mason, T. O.; Perkins, J. D.; Ginley, D. S. *Electrochem. Soc. Proc.* **1999**, 274. (c) Kawamura, K.; Takahashi, M.; Yagihara, M.; Nakayama, T. Eur. Pat. Appl. EP 1271561, A2 20030102, CAN 138:81680, AN 2003:4983, 2003.

(4) (a) Kammler, D. R.; Mason, T. O.; Young, D. L.; Coutts, T. J.; Ko, D.; Poeppelmeier, K. R.; Williamson, D. L. *J. Appl. Phys.* **2001**, *90*, 5979. (b) Zhao, Z. Y.; Morel, D. L.; Ferekides, C. S. *Thin Solid Films* **2002**, *413*, 203.

(5) (a) Babcock, J. R.; Wang, A. C.; Metz, A. W.; Edleman, N. L.; Metz, M. V.; Lane, M. A.; Kannewurf, C. R.; Marks, T. J. *Chem. Vap. Deposition* **2001**, *7*, 239. (b) Asahi, R.; Wang, A.; Babcock, J. R.; Edleman, N. L.; Metz, A. W.; Lane, M. A.; Dravid, V. P.; Kannewurf, C. R.; Freeman, A. J.; Marks, T. J. *Thin Solid Films* **2002**, *411*, 101.

(6) Wang, A.; Babcock, J. R.; Edleman, N. L.; Metz, A. W.; Lane, M. A.; Asahi, R.; Dravid, V. P.; Kannewurf, C. R.; Freeman, A. J.; Marks, T. J. *Proc. Natl. Acad. Sci. U.S.A.* **2001**, *98*, 7113.

(7) Yan, M.; Lane, M.; Kannewurf, C. R.; Chang, R. P. H. *Appl. Phys. Lett.* **2001**, *78*, 2342.

(8) (a) Coutts, T. J.; Young, D. L.; Li, X.; Mulligan, W. P.; Wu, X. *J. Vac. Sci. Technol., A: Vac., Surf., Films* **2000**, *18*, 2646. (b) Wu, X.; Coutts, T. J.; Mulligan, W. P. *J. Vac. Sci. Technol., A: Vac., Surf., Films* **1997**, *15*, 1057.

(9) Koffyberg, F. P. *Phys. Rev. B* **1976**, *13*, 4470.

tion-dependent Burstein−Moss (B−M) energy level shift.[10] CdO, with a simple cubic rock salt structure, broadly dispersed s-like conduction bands, and a small carrier effective mass, is seen to represent an ideal model material in which to study the effects of doping on TCO band structure, crystal chemistry, and charge transport.

In our previous work, undoped and doped CdO thin films were successfully grown by MOCVD using optimized metal−organic Cd precursors.[5,6] In-doped CdO thin films grown on glass by MOCVD exhibit conductivities as high as 16800 S/cm.[6] It was found that In doping dramatically alters the CdO band structure by extensive mixing of In 5s and Cd 5s states, also yielding a hybridization gap in the conduction band. Our continued interest in CdO-based TCOs focuses on understanding crystal structure−charge transport relationships by doping CdO with a wide variety of dopants which (1) offer controlled lattice parameter excursions via varying ionic radius, (2) offer varying degrees of orbital overlap between Cd^{2+} conduction band states and dopant ions, and (3) contribute varying formal numbers of conduction band electrons to increase the effective carrier density by substituting for Cd^{2+}. For all these reasons, Sc^{3+} with a six-coordinate ionic radius of 0.89 Å,[11] which is substantially smaller than that of Cd^{2+}, 1.09 Å, would be of great interest in the study of dopant size effects. In addition, compared with In^{3+} and Sn^{4+}, Sc^{3+} does not have an energetically comparable s state that can hybridize with the Cd 5s states in the conduction band.[12] Hence, Sc-doped CdO would also be of great interest to probe orbital hybridization effects by comparison with the corresponding In- and Sn-doped CdO thin films.

In this paper, we report the growth of Sc-doped CdO (CSO) thin films on amorphous glass and single-crystal MgO(100) by MOCVD. The CSO thin film phase structure, microstructure, and electrical and optical properties are investigated in detail. In addition, we report first-principles full-potential linear augmented plane wave (FLAPW)[5b,6,13] electronic band structure calculations within the screened-exchange local density approximation (sX-LDA) to treat both the ground and the excited states, which allow us to compare and contrast the structural, electronic, and optical properties of In- and Sc-doped CdO systems. It is found both experimentally and theoretically that (as might, a priori, be expected) Sc doping shrinks the CdO lattice parameter substantially due to its smaller ionic radius. As-deposited CSO thin films are highly conductive and transparent, with an average transmittance >80% in the visible range. Thin film conductivities as high as 18100 S/cm on MgO(100) are obtained at the optimum Sc doping level of 1.8 atom %. This conductivity is roughly 5 times greater than that of commercial ITO.

Experimental Section

MOCVD Precursors and Thin Film Growth. The volatile metal−organic Cd precursor $Cd(hfa)_2$(*N*,*N*-DE-*N*′,*N*′-DMEDA) (**1**) (hfa = hexafluoroacetylacetonate; *N*,*N*-DE-*N*′,*N*′-DMEDA = *N*,*N*′-diethyl-*N*,*N*′-dimethylethylenediamine) was prepared from high-purity $Cd(NO_3)_2 \cdot 4H_2O$ (99.999%, Aldrich),[14] and was triply vacuum-sublimed. $Sc(dpm)_3$ (**2**) (dpm = dipivaloylmethanate) was prepared from Sc_2O_3 (99.99%, Alfa Aesar) by a literature procedure.[15]

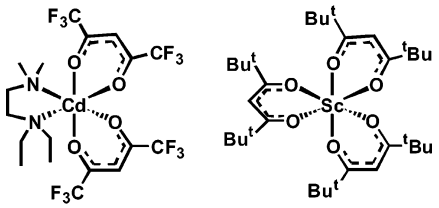

1 **2**

CSO thin film growth was carried out in a previously described horizontal, cold-wall MOCVD reactor.[16] For CdO and Sc-doped CdO thin film growth, the precursor reservoir temperatures/Ar carrier gas flow rates were optimized at (**1**) 85 °C/15 sccm and (**2**) 110 °C/5−50 sccm. The O_2 oxidizing gas was introduced upstream at 400 sccm after bubbling through distilled water. A system operating pressure of 4.0 ± 0.1 Torr and a substrate temperature of 400 °C was maintained during the thin film deposition. Corning 1737F glass and polished single-crystal MgO(100) (a = 4.216 Å) substrates were purchased from Precision Glass and Optics and MTI Corp., respectively. Both the glass and the MgO(100) substrate surfaces were cleaned with acetone prior to the film deposition, and were placed side-by-side on a SiC-coated susceptor in the growth reactor for simultaneous growth experiments.

Film Physical Characterization Measurements. Composition analyses were carried out using inductively coupled plasma atomic emission spectrometry (ICP-AES). Fluorine and carbon contamination (atom %) were quantitatively analyzed using an Omicron ESCA probe X-ray photoelectron spectrometer. Optical transparency measurements were carried out in the range of 300−3300 nm with a Cary 500 UV−vis−near-IR spectrophotometer. Film thicknesses were measured using a Tencor P-10 profilometer after a step in the film was etched using 5% HCl solution. X-ray diffraction $\theta-2\theta$ scans of CdO films on glass were obtained with a Rigaku DMAX-A powder diffractometer using Ni-filtered Cu Kα radiation. Rocking curves and ϕ scans of the epitaxial thin films on MgO(100) substrates were obtained on a home-built Rigaku four-circle diffractometer with detector-selected Cu Kα radiation. Film surface morphology was imaged using a Digital Instruments Nanoscope III atomic force microscope operating in the contact mode. Film microstructure was imaged on a Hitachi S4500 FE scanning electron microscope. Ambient-temperature four-probe charge transport data were acquired on a Bio-Rad HL5500 Hall-effect measurement system. Variable-temperature Hall-effect and four-probe conductivity data were collected between 77 and 330 K using the instrumentation described previously.[17]

Theoretical Methods

First-principles electronic band structure calculations were performed using the highly precise all-electron FLAPW method[13] that has no shape approximation for the potential and charge density. The exchange-correlation energies were treated via the LDA. Cutoffs of the plane-wave basis (14.4 Ry) and potential representation (81.0 Ry) and expansion in terms of spherical harmonics with $l \leq 8$ inside the muffin-tin spheres were used. To overcome the shortcomings of LDA for the determination of the excited-state band structure and optical properties

(10) Burstein, E. *Phys. Rev.* **1954**, *93*, 632.
(11) Shannon, R. D. *Acta Crystallogr.* **1976**, *A32*, 751.
(12) Medvedeva, J. E.; Freeman, A. J. To be published.
(13) Wimmer, E.; Krakauer, H.; Weinert, M.; Freeman, A. J. *Phys. Rev. B* **1981**, *24*, 864.
(14) Metz, A. W.; Ireland, J. R.; Zheng, J. G.; Lobo, R. P. S. M.; Yang, Y.; Ni, J.; Stern, C. L.; Dravid, V. P.; Bontemps, N.; Kannewurf, C. R.; Poeppelmeier, K. R.; Marks, T. J. *J. Am. Chem. Soc.* **2004**, *126*, 8477.
(15) Fleeting, K. A.; Davies, H. O.; Jones, A. C.; O'Brien, P.; Leedham, T. J.; Crosbie, M. J.; Wright, P. J.; Williams, D. J. *Chem. Vap. Deposition* **1999**, *5*, 261.
(16) Hinds, B. J.; McNeely, R. J.; Studebaker, D. B.; Marks, T. J.; Hogan, T. P.; Schindler, J. L.; Kannewurf, C. R.; Zhang, X. F.; Miller, D. J. *J. Mater. Res.* **1997**, *12*, 1214.
(17) Lyding, J. W.; Marcy, H. O.; Marks, T. J.; Kannewurf, C. R. *IEEE Trans. Instrum. Meas.* **1988**, *37*, 76.

of CSO, we used the self-consistent sX-LDA method[18] with cutoff parameters of 10.24 Ry in the wave vectors and $l \leq 3$ inside the muffin-tin spheres. Summations over the Brillouin zone were carried out using 10 special k points in the irreducible wedge.

Results and Discussion

We first describe a simple, effective, low-pressure MOCVD growth process for Sc-doped CdO (CSO) thin films. Then, CSO film composition, morphology, microstructure, and epitaxy are characterized as a function of doping level using a broad array of complementary physical techniques. In addition, the optical and electrical properties of as-deposited CSO thin films are investigated in detail, and microstructure−charge transport−optical properties relationships discussed. Finally, band structure calculations using the highly precise sX-LDA formalism are used to help understand CSO structural, electronic, and optical properties.

Film Growth. A series of CSO thin films was grown on 1737 F glass and single-crystal MgO(100) at 400 °C by low-pressure MOCVD using the metal−organic Cd precursor **1** and the Sc precursor **2**. Thin films with a thickness of ∼180 nm on glass and ∼350 nm on MgO(100) are obtained after 2 h of growth, at a growth rate of ∼1.5 nm/min on glass and ∼3 nm/min on MgO(100). The CSO thin film growth rate on single-crystal MgO(100) is more rapid than that on amorphous glass substrates, presumably due to epitaxy effects. Film growth is found to be very sensitive to the substrate temperature and O_2 partial pressure. At a given Cd precursor delivery rate (precursor temperature/Ar carrier gas flow rate of 85 °C/15 sccm), the film growth rate decreases with increasing substrate temperature over the range 300−400 °C. This is because CdO itself is relatively volatile,[19] leading to competition between the CdO film deposition and evaporation on the substrate at higher temperatures. Films could only be deposited at temperatures below 425 °C under the present reactor conditions. More importantly, low precursor delivery rates proved to be highly effective in obtaining highly epitaxial thin films (see below). In addition, as-deposited films grown at low delivery rates (≤1.5 nm/min) exhibit larger grain sizes and higher measured mobilities (see below) than films grown at higher delivery rates (>1.5 nm/min). These as-grown films are uniformly pale-yellow in color but exhibit good optical transparency. The Sc doping level can be incrementally varied from 0.7 to 15 atom % by varying the Ar carrier gas flow rate and reservoir temperature of the Sc precursor.

Film Composition, Morphology, Microstructure, and Epitaxy. Fluorine and carbon contamination in the CSO films was quantitatively investigated by X-ray photoelectron spectroscopy (XPS) due to the use of a F-containing Cd−organic MOCVD precursor. To analyze the film composition, the surface layer (∼3−5 nm) exposed to air was first removed by Ar ion sputtering (2 kV, 10 μA; sputtering rate ∼3 Å/min). There are no detectable changes in the composition or the chemical state of the Cd, Sc, and O constituents after 10, 20, and 40 min of sputtering. Less than 0.5 atom % F and 2.5 atom % C are detected in the as-deposited CSO thin films, and hence, F introduction is minimal and should not contribute significantly as a doping mechanism for the high conductivity. Previous SIMS analyses on CdO films grown under similar MOCVD conditions using an analogous hfa precursor indicated F levels of 0.26 atom %.[14]

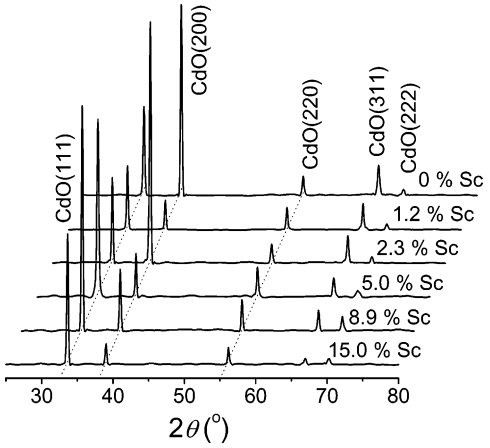

Figure 1. $\theta-2\theta$ X-ray diffractograms of CSO thin films grown on glass at 400 °C by MOCVD as a function of Sc doping level (atom %).

X-ray diffraction $\theta-2\theta$ scans of CSO thin films grown on glass were carried out between $2\theta = 25°$ and $2\theta = 80°$. Figure 1 shows the XRD data as a function of Sc doping level. All of the films are phase-pure and polycrystalline, with the fcc CdO structure.[20] No Sc_2O_3[21] or other contaminating phases are detected by XRD, even at the 15 atom % Sc doping level, indicating that Sc^{3+} substitutes uniformly for Cd^{2+} in the lattice rather than forming a second phase. It is clear that the presently determined solubility of Sc in CdO thin films is ≥15 atom %. In contrast to the present polycrystalline microstructures of the MOCVD-derived CSO thin films grown on amorphous glass substrates, all the epitaxial CSO thin films grown on single-crystal MgO(100) exhibit a highly (200) textured microstructure, even though the lattice mismatch between the MgO(100) substrate and CdO crystal structure is 10.2%. The textured structure of the as-deposited thin films was further assessed by rocking curves and ϕ-scans (Figure 2). The rocking curves of the films show good out-of-plane alignment (Figure 2A). The full width at half-maximum (fwhm) is increased from 0.5° for undoped CdO films to 1.5° for CSO at 6.4 atom % Sc doping, suggesting that the crystallite alignment decreases slightly with increased Sc doping. The in-plane orientation was also investigated by ϕ-scans of the CdO(111) reflection at $\chi = 54.7°$ (Figure 2B). The clear 4-fold rotational symmetry of the CdO(111) reflections along with the small fwhms (0.5° for pure CdO, 0.7° for CSO at 1.8 atom % Sc doping) reveals excellent in-plane orientation of the films. The orientation relation between CSO thin films and the MgO(100) substrates is therefore CdO(100)||MgO(100).

Using polycrystalline silicon as an internal calibration reference, the precise lattice parameters of the MOCVD-derived CSO thin films on glass were calculated. It is found that the lattice parameters decrease linearly with increasing Sc doping level (Figure 3), indicating that the lattice dimensions contract monotonically with the introduction of Sc^{3+}, having a smaller six-coordinate ionic radius, 0.89 Å, vs 1.09 Å for Cd^{2+}. In addition, the lattice parameters of the CSO films on MgO(100)

(18) Asahi, R.; Mannstadt, W.; Freeman, A. J. *Phys. Rev. B* **1999**, *59*, 7486 and references therein.
(19) Lamoreaux, R. H.; Hildenbrand, D. L.; Brewer, L. *J. Phys. Chem. Ref. Data*, **1987**, *16*, 419.
(20) JCPDS-International Centre for Diffraction Data, CdO: 05-0640.
(21) JCPDS-International Centre for Diffraction Data, Sc_2O_3: 05-0629.

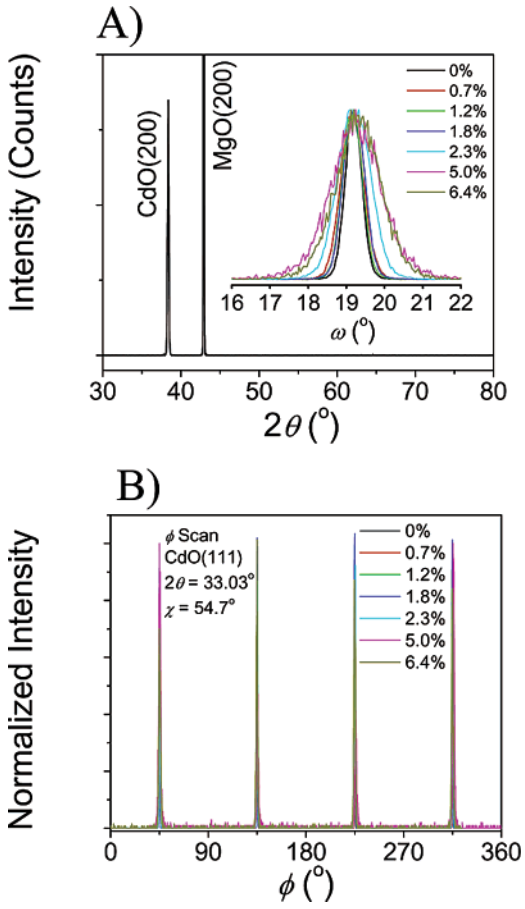

Figure 2. XRD texture analyses of CSO thin films grown on MgO(100) by MOCVD as a function of Sc doping level: (A) $\theta-2\theta$ X-ray diffractograms (inset: rocking curves measured on the CdO(200) XRD peak); (B) in-plane ϕ-scans measured on the CdO(111) XRD peak with $\chi = 54.7$. The Sc doping level is given in atom percent.

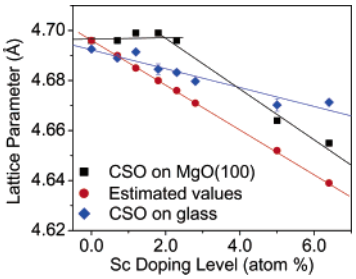

Figure 3. Lattice parameter changes as a function of Sc doping level for CSO thin films. Estimated Vegard's law lattice parameter values are calculated according to the following equation: $a_{estimated} = a_{CdO}[(r_{Cd}(Cd\%) + r_{Sc}(Sc\%))/(r_{Cd})]$, where a_{CdO} is the CdO lattice parameter (4.696 Å), r_{Cd} is the six-coordinate ionic radius of Cd, Cd% is the Cd atomic percentage, r_{Sc} is the six-coordinate ionic radius of Sc, and Sc% is the Sc atomic percentage (Cd% + Sc% = 1). Lines through the data points are drawn as a guide to the eye.

were calculated using the MgO(200) reflection as an internal reference. When Sc^{3+} doping is ≤2.8 atom %, there is no significant change in lattice parameters, doubtless reflecting epitaxy effects. However, the lattice parameters decrease precipitously with further Sc^{3+} doping, reaching 4.653 Å at 6.4 atom % doping (Figure 3). It will be seen below that these results are in good agreement with the FLAPW calculations. Ambrosini et al. observed a similar lattice shrinkage trend upon introducing Sc into bulk In_2O_3 samples.[22] However, the shrinkage is not as large as estimated from a simple Vegard's law weighted average

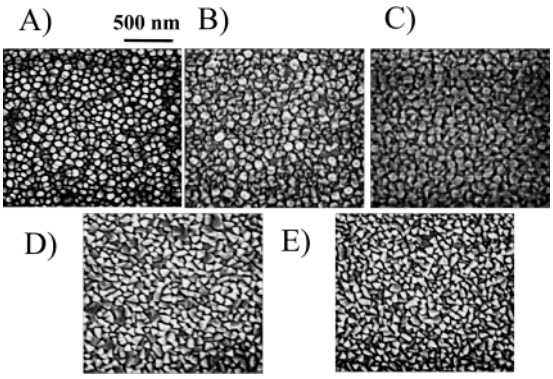

Figure 4. SEM images of CSO thin films on glass as a function of Sc doping level (atom %): (A) 0.0; (B) 1.2; (C) 2.3; (D) 5.0; (E) 6.4.

of the Sc^{3+} and Cd^{2+} ionic radii (Figure 3).[23] One possible explanation is that some of the Sc^{3+} dopant ions exist as interstitial ions instead of directly substituting for Cd^{2+} in the lattice. Another possibility is that the Sc^{3+}-induced doping shrinkage is compensated by an expansion mechanism which originates from the antibonding character of the conduction band formed from Cd 5s and O 2p states. This interesting phenomenon was proposed for In- and Y-doped CdO bulk materials by Morozova et al.,[24] and Dou et al.,[25] who reported that the In- and Y-doped CdO lattice parameters increase with increasing doping levels, even though the dopant ions, In^{3+} and Y^{3+} (radii of 0.94 and 1.04 Å, respectively), are again smaller than Cd^{2+}. This issue will be discussed further in the theory section (Band Structure Calculations). Besides these possibilities, an expansion mechanism involving Cd^{2+} reduction to Cd^{+} that could compensate for the Sc^{3+}-induced doping shrinkage was proposed by Cimino et al.[26] This issue will also be discussed below.

The surface morphologies of the as-deposited CSO thin films were examined by scanning electron microscopy (SEM) and atomic force microscopy (AFM). SEM surface images show that the as-deposited thin films on glass are densely packed with a grained structure (Figure 4). At low doping levels, the films on glass have grains with rounded shapes. As the doping levels increase to greater than 2.8 atom %, the grains of the films on glass become triangular in shape, consistent with high in-plane order and with (111) planes parallel to the surface, in agreement with the above XRD analysis (Figure 1). The thin films on glass exhibit a root-mean-square (RMS) roughness ranging from 4.5 to 8.2 nm over a 25 μm^2 area (Figure 5A), as determined by contact mode AFM. The average grain size of the films on the glass is 100−150 nm (Figure 5A). Low doping level (<2 atom %) films on MgO(100) are featureless by SEM, and their surface morphology is found to be very smooth and uniform by AFM (Figure 5B). The RMS roughness of the films on MgO(100) ranges from 1.6 to 1.9 nm at low doping levels (<2 atom %), indicating that the CSO thin films grown on MgO(100), with a nearly single grained structure, are significantly smoother than CSO films grown on glass substrates.

(22) Ambrosini, A.; Duarte, A.; Poeppelmeier, K. R.; Lane, M.; Kannewurf, C. R.; Mason, T. O. *J. Solid State Chem.* **2000**, *153*, 41.
(23) Vegard, L. *Z. Phys.* **1921**, *5*, 17.
(24) Morozova, L. V.; Komarov, A. V. *Russ. J. Appl. Chem.* **1995**, *68*, 1240.
(25) (a) Dou, Y.; Egdell, R. G.; Walker, T.; Law, D. S. L.; Beamson, G. *Surf. Sci.* **1998**, *398*, 241. (b) Dou, Y.; Fishlock, T.; Egdell, R. G.; Law, D. S. L.; Beamson, G. *Phys. Rev. B* **1997**, *55*, 13381.
(26) Cimino, A.; Marezio, M. *J. Phys. Chem. Solids* **1960**, *17*, 57.

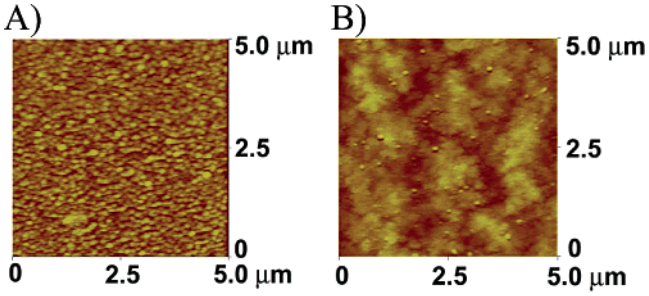

Figure 5. AFM images of 2.3 atom % Sc-doped CdO thin films: (A) on glass; (B) on MgO(100).

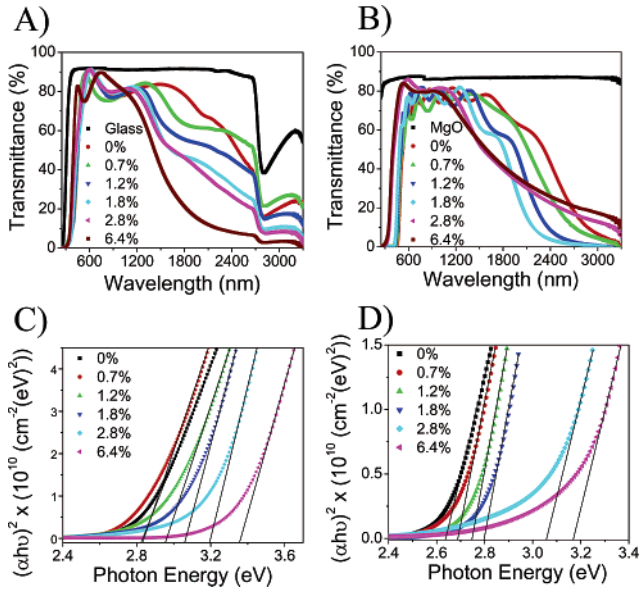

Figure 6. Optical characterization of CSO thin films as a function of Sc doping: (A) optical transmission spectra of CSO on glass; (B) optical transmission spectra of CSO on MgO(100); (C) band gap estimations of CSO on glass; (D) band gap estimations of CSO on MgO (100). Sc doping levels are given in atom percent.

Film Optical and Electrical Properties. The as-grown CSO films are pale-yellow but highly transparent. The color of the CSO films becomes lighter with increased Sc^{3+} doping as the band edge shifts to higher energies. CSO thin films with thicknesses of 180 nm on glass and 350 nm on MgO(100) exhibit an average transmittance at 550 nm of ≥80% (Figure 6A,B). As the Sc doping level increases, the band edges blue-shift dramatically, doubtless due to the B−M band-filling effect.[10] Band gap estimates were derived from the optical transmittance spectra by extrapolating the linear portion of the plot of $(\alpha h\nu)^2$ vs $h\nu$ to $\alpha = 0$ (Figure 6C,D). The band gap increases from 2.7 to 3.4 eV with an increase in Sc^{3+} doping. Simultaneously, the plasma edge shifts to the blue due to the increased free carrier scattering with the increased levels of Sc doping.

All CSO thin films exhibit n-type conductivity as determined by negative Hall coefficients. The charge transport properties of the as-grown thin films as a function of Sc doping are shown in Figure 7. For undoped CdO thin films, carrier mobilities as high as 141 and 217 $cm^2/(V\cdot s)$ are achieved on glass and MgO-(100), respectively, which are more than 5 times greater than those of commercial ITO films. With increased Sc doping, the carrier concentration increases from 2.3 × 10^{20} for undoped CdO thin films on glass to 6.7 × 10^{20} at ∼5.0 atom % Sc

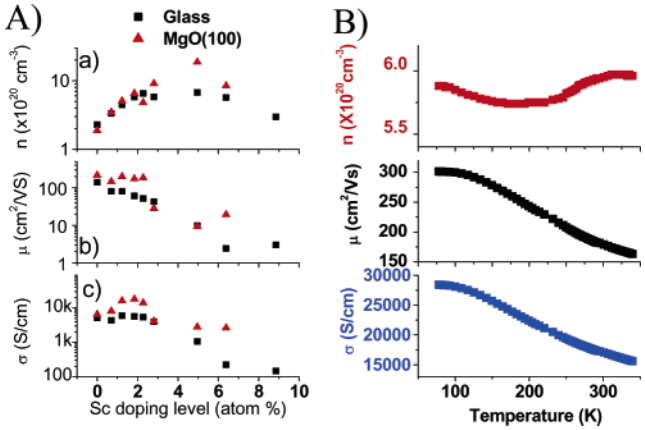

Figure 7. (A) Room-temperature four-probe charge transport measurements for CSO thin films on glass and MgO(100): (a) carrier concentration; (b) mobility; (c) conductivity. (B) Variable-temperature conductivity and Hall-effect measurements for a 1.8 atom % CSO thin film on MgO(100).

doping. On MgO(100) substrates, the carrier concentration increases from 1.9 × 10^{20} for pure CdO thin films to 18.7 × 10^{20} at ∼5.0 atom % Sc doping. This indicates that most of the Sc^{3+} substitutes uniformly for Cd^{2+} in the lattice as an effective n-type dopant rather than forming a second phase. Beyond 5.0 atom % Sc doping, the carrier concentration does not increase with increasing Sc doping, suggesting that some Sc^{3+} may exist as interstitial ions or as free scandium oxide, which, however, is still below the XRD detection limit. The mobility, however, drops rapidly with increased Sc^{3+} doping. Compared to In-doped CdO on glass,[5,6] the present CSO thin films on glass exhibit lower carrier mobilities and concentrations, likely due to the lack of significant orbital hybridization between the Cd 5s conduction band and the Sc 4s states (see more below).

Thin films with conductivities of 6000 and 18100 S/cm on glass and MgO(100), respecitively, are achieved at ∼1.2 atom % Sc doping on glass and 1.8 atom % Sc doping on MgO-(100). Compared to films on glass, CSO films on MgO(100) at the same Sc doping level and with similar grain sizes exhibit much greater carrier mobilities and carrier concentrations (Figure 7), arguing that the highly textured structure possesses fewer scattering centers and greater doping efficiency. When Sc^{3+} doping levels are greater than ∼2.8 atom %, the carrier concentration plateaus and the mobilities decline precipitously. Although the lattice parameters are further compressed, the increased doping does not contribute additional free carriers. This explanation is consistent with the plasma edge trend: at the highest doping levels, further blue-shifting of the plasma edges is negligible.

Figure 7B shows the temperature dependence of CSO film charge transport properties obtained from four-probe conductivity and Hall-effect measurements for a 1.8 atom % Sc-doped film on MgO(100), which achieves the highest conductivity of 18100 S/cm at room temperature. In the low-temperature region (<100 K), the mobility and conductivity are essentially independent of temperature, suggesting that neutral impurity scattering (NIS) and/or ionized impurity scattering (IIS) are dominant (the former mechanism is supported by the mobility vs carrier concentration results of Figure 7).[14,26,27] In the high-

(27) (a) Dingle, R. B. *Philos. Mag.* **1955**, *46*, 831. (b) Erginsoy, C. *Phys. Rev.* **1950**, *79*, 1013. (c) Frank, G.; Koestlin, H. *Appl. Phys. A: Solids Surf.* **1982**, *A27*, 197.

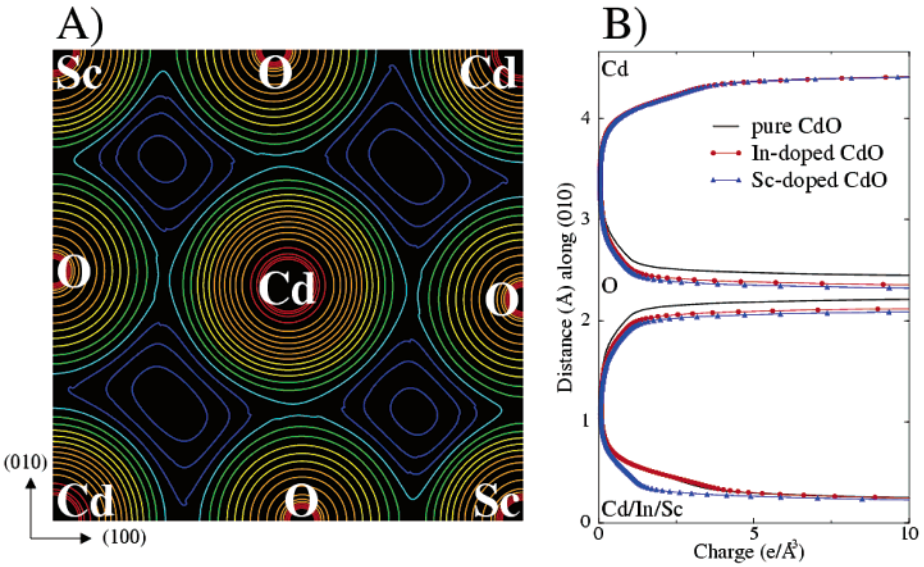

Figure 8. (A) Calculated charge density distribution for 12.5 atom % Sc-doped CdO in the *ab* plane. (B) Comparison of the charge density along (010) for pure and Sc (or In) doped cases. Results for pure CdO and 12.5 atom % In-doped CdO were obtained from additional calculations.

temperature range (>100 K), the mobility and conductivity decrease significantly with increasing temperature, reminiscent of metal-like character, and suggesting that lattice vibration scattering (LVS) has now become an important scattering contributor.[28,29,30a] In the present study, the highly textured epitaxial CSO thin films grown on MgO(100), having carrier concentrations higher than and grain sizes similar to those of films grown in parallel on glass, possess significantly higher carrier mobilities, which is most likely attributable to a reduction in NIS caused by improved epitaxy-induced crystallinity.[14] The importance of grain boundary scattering (GBS) is an incompletely resolved mechanistic issue in most CdO-based TCOs. It has been argued that GBS is insignificant because the carrier mean-free paths of highly degenerate TCOs are typically much smaller than the grain sizes of typical films.[26,28,30] Our recent microstructure−charge transport−optical reflectivity results on undoped MOCVD-derived CdO thin films also argue that GBS is not a dominant process, even in high-quality epitaxial CdO films with modest carrier concentrations and small grain sizes, 2×10^{20} cm^{-3} and ~100 nm, respectively.[14] However, it is conceivable that reduced large-angle grain boundary scattering and better intergrain contact in the epitaxial thin films, due to the highly ordered grain alignment, may contribute in some degree to the greater observed carrier mobilities.

Band Structure Calculations. The FLAPW total energy full structure optimization for CSO was performed at 12.5 atom % Sc doping. The lattice parameter, *a*, and the internal structure relaxation due to the Sc doping were first calculated. The smaller lattice parameter of CSO found at 12.5 atom % doping, $a = 4.63$ Å, than that of pure CdO (4.66 Å, obtained from a separate calculation) is found to be in agreement with the experimental findings discussed above. From similar band structure calculations for Ga-, Sc-, In-, and Y-doped CdO to be discussed elsewhere,[12] we find that a smaller dopant ionic radius results in weaker Cd 5s−O 2p hybridization due to relaxation of the oxide anions around the dopant cations. Therefore, in the case of In^{3+} and Y^{3+}, whose ionic radii are relatively close to that of Cd^{2+}, the antibonding expansion mechanism is dominant, while Sc^{3+} has a sufficiently small ionic radius to weaken the s−p hybridization and, hence, to compress the lattice. In addition, the reduced ionic radius of Sc and the oxygen relaxation are clearly seen in the calculated FLAPW charge density distribution plot (Figure 8). Note here that we find negligible changes in the effective ionic radius of Cd for dopant concentrations as large as 12.5 atom % (Figure 8), so that the reduction from Cd^{2+} to Cd^{+} as proposed by Cimino et al.[26] seems unlikely.

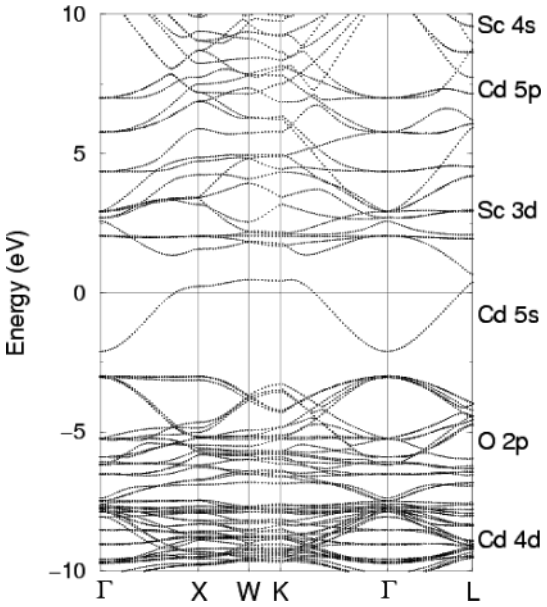

Figure 9. Calculated sX-LDA band structure for 12.5 atom % Sc-doped CdO along the high-symmetry directions in the Brillouin zone. The origin of the energy is taken at the Fermi level; the electronic states are labeled.

The band structure of CSO at 12.5 atom % Sc doping calculated within the sX-LDA method is shown in Figure 9. The prominent, highly dispersed single band, derived mainly

(28) Chen, M.; Pei, Z. L.; Wang, X.; Yu, Y. H.; Liu, X. H.; Sun, C.; Wen, L. S. *J. Phys. D: Appl. Phys.* **2000**, *33*, 2538.
(29) Bardeen, J.; Shockley, W. *Phys. Rev.* **1950**, *80*, 72.
(30) (a) Zhang, D. H.; Ma, H. L. *Appl. Phys. A: Solids Surf.* **1996**, *A62*, 487. (b) Gilmore, A. S.; Al-Kaoud, A.; Kaydanov, V.; Ohno, T. R. *Mater. Res. Soc. Symp. Proc.* **2001**, *666*, F3.10/1. (c) Tahar, R. B. H.; Tahar, N. B. H. *J. Appl. Phys.* **2002**, *92*, 4498.

from the 5s states of Cd, crosses the Fermi level in the [100] (Δ), [110] (Σ), and [111] (Λ) directions. Similar electronic features were obtained[6] for In-doped CdO. However, in marked contrast to the case of In doping, the Sc 4s states in CSO are found to lie high up in the conduction band (at ~9.5 eV) and so do not hybridize with the Cd 5s states. On the other hand, the free-electron-like band is now separated away from the Sc 3d states by a second band gap (Figure 9) which effectively decreases the dispersion of the s-type band. Indeed, we find that in CSO the width of the dispersed band (2.6 eV) is ~1 eV narrower than that in the In-doped CdO.[5b,6,12] Together with the lack of hybridization between Cd 5s and Sc 4s states, this convincingly explains the observed lower carrier mobilities in Sc-doped CdO as compared to the In-doped CdO materials. Finally, we find that the Sc doping results in a Burstein−Moss shift which significantly widens the optical transparency window, in agreement with the experimental results discussed above. As expected, the LDA is found to underestimate the band gap energies which determine optical transparency in the visible range, yielding 2.27, 2.89, and 2.92 eV in the [100], [110], and [111] directions, respectively. Strikingly, the calculated sX-LDA band gap energies are found to be 3.02, 3.65, and 3.76 eV in the [100], [110], and [111] directions, respectively—in good agreement with the present experimental optical band gap energy (3.4 eV).

Conclusions

Highly conductive and transparent CSO thin films have been grown on glass and single-crystal MgO(100) substrates at 400 °C by an MOCVD process. XRD data reveal that all of these as-deposited CSO films are phase-pure and highly crystalline, with features assignable to the cubic CdO-type crystal structure. CdO lattice dimensions are found to contract with the introduction of Sc^{3+}, in agreement with the FLAPW calculations. However, the observed lattice shrinkage is to some degree compensated by an expansion mechanism, which, on the basis of our band structure calculations for Ga-, Sc-, In-, and Y-doped CdO, originates from the antibonding character of the conduction band formed from the Cd 5s and O 2p states. Thin film conductivities as high as 6000 S/cm are obtained on glass substrates at 1.2 atom % Sc doping. Compared to In-doped CdO, the CSO films on glass exhibit lower carrier mobilities and concentrations, due to the lack of energetically comparable Sc s states that can hybridize with the Cd 5s conduction band and the lower dispersion of this s-type band—as revealed by first-principles FLAPW electronic band structure calculations. CSO thin films on MgO(100) with a maximum conductivity of 18100 S/cm are obtained at a Sc doping level of ~1.8 atom %, which is to date the most conductive transparent conducting oxide material grown by MOCVD. These epitaxial films grown on MgO(100) exhibit a biaxial, highly textured microstructure, leading to higher doping efficiency than on glass and with fewer scattering centers. This is likely responsible for the higher conductivity compared to that of the films on glass. All of these MOCVD-derived thin films exhibit good optical transparency, with an average transmittance ≥80% in the visible range. Sc doping widens the band gap from 2.7 to 3.4 eV via a Burstein−Moss band-filling shift, in agreement with sX-LDA calculations. The high electrical conductivity and optical transparency render MOCVD-derived CSO thin films attractive candidates for next-generation transparent electrodes for a variety of optoelectronic devices.

Acknowledgment. This work was supported by the United States Display Consortium (USDC), the NSF (Grant CHE-0201767), and the NSF-MRSEC program (Grant DMR-00760097) at the Northwestern Materials Research Center. We thank Dr. J. Carsello for his assistance with X-ray diffraction measurements and Dr. N. Wu for his assistance with XPS measurements at Keck-II/NUANCE facility.

JA0467925